

# Identification of the Long-Sought Common-Envelope Events.

N. Ivanova<sup>1\*</sup>, S. Justham<sup>2</sup>, J.L. Avendano Nandez<sup>1</sup> & J.C. Lombardi Jr.<sup>3</sup>

<sup>1</sup>Dept. of Physics, University of Alberta, Edmonton, AB, T6G 2E7, Canada,

<sup>2</sup>National Astronomical Observatories, The Chinese Academy of Sciences, Beijing 100012, China,

<sup>3</sup>Department of Physics, Allegheny College, Meadville, PA 16335, USA

\*To whom correspondence should be addressed. E-mail: nata.ivanova@ualberta.ca.

**Common-envelope events (CEEs), during which two stars temporarily orbit within a shared envelope, are believed to be vital for the formation of a wide range of close binaries. For decades, the only evidence that CEEs actually occur has been indirect, based on the existence of systems that could not be otherwise explained. Here we propose a direct observational signature of CEE arising from a physical model where emission from matter ejected in a CEE is controlled by a recombination front as the matter cools. The natural range of timescales and energies from this model, as well the expected colors, light-curve shapes, ejection velocities and event rate, match those of a recently-recognized class of red transient outbursts.**

Many binary star systems, including X-ray binaries, cataclysmic variables, close double-neutron stars, and the potential progenitors of Type Ia supernovae and short-duration  $\gamma$ -ray bursts, are thought to be formed by CEEs. Because most stellar-mass binary merger sources for gravitational waves have experienced a CEE in their past, improved knowledge of CEEs should decrease the large uncertainty in theoretically-predicted merger rates. However, the short timescale expected for CEEs suggested that we would never directly observe them, allowing us only to draw inferences from the systems produced.

A CEE begins when a binary orbit becomes unstable and decays. This might, for example, be driven purely by tidal forces (i.e. the Darwin instability), although CEEs are more commonly imagined as following a period of rapid mass transfer from one star to the other (1). In some cases the rate of transfer is so high that the receiving star is unable to accrete all the matter without forming a shared common envelope (CE) around the binary. This CE causes drag on one or both stars and hence orbital decay, with orbital energy and angular momentum

being transferred to the CE. This may end with a stellar merger or – if the CE is ejected – the binary can survive, typically with a much reduced orbital separation, critical to explaining many observed compact binaries.

When a CEE results in formation of a close binary, it is expected that a substantial proportion of the mass is ejected – typically almost the entire envelope of one of the stars. Some mass can also be ejected in the case of a merger. This partial ejection has two causes (2). Firstly, the orbital energy deposited into the CE early in the merger may exceed the binding energy of the outer layers. Secondly, the upper layers of the envelope absorb a substantial amount of the orbital angular momentum of the companion, and angular momentum transport may be too slow to share this across the envelope as a whole.

Here we consider the behavior of this ejected matter to try to predict the appearance of CEEs. A situation involving similar physics – type IIP supernovae – has been previously studied (e.g, (3–5)). In that model, as the ejected stellar plasma expands and cools, recombination changes its opacity, leading to the propagation of a photosphere-defining “cooling wave,” which moves inwards with respect to the mass variable.

For smooth and spherically-symmetric ejecta distributions, the model light-curve will have a plateau shape: the area of the photosphere is defined by recombination, and so the emitting surface does not grow with the speed at which the ejected matter itself moves. During this phase, whilst material ejected by the CEE will expand with velocity of the order of magnitude of the initial escape velocity, the photospheric radius should appear almost constant. The luminosity  $L_P$  of the emission during the plateau (3–5), re-scaled to the likely energy range of CEE, is

$$L_P \approx 1.7 \times 10^4 L_\odot \left( \frac{R_{\text{init}}}{3.5R_\odot} \right)^{2/3} \left( \frac{E_k^\infty}{10^{46}\text{erg}} \right)^{5/6} \left( \frac{m_{\text{unb}}}{0.03M_\odot} \right)^{-1/2} \left( \frac{\kappa}{0.32\text{cm}^2\text{g}^{-1}} \right)^{-1/3} \left( \frac{T_{\text{rec}}}{4500\text{K}} \right)^{4/3} \quad (1)$$

where  $R_{\text{init}}$  is the initial radius,  $E_k^\infty$  is the kinetic energy that the unbound mass  $m_{\text{unb}}$  has at late times after escaping the potential well,  $\kappa$  is the opacity of the ionized ejecta, and  $T_{\text{rec}}$  is the recombination temperature. The duration of the plateau  $t_P$  with the same assumptions is

$$t_P \approx 17 \text{ days} \left( \frac{R_{\text{init}}}{3.5R_\odot} \right)^{1/6} \left( \frac{E_k^\infty}{10^{46}\text{erg}} \right)^{-1/6} \left( \frac{m_{\text{unb}}}{0.03M_\odot} \right)^{1/2} \left( \frac{\kappa}{0.32\text{cm}^2\text{g}^{-1}} \right)^{1/6} \left( \frac{T_{\text{rec}}}{4500\text{K}} \right)^{-2/3} \quad (2)$$

This model does not depend on the origin of the energy released during the outburst. For type IIP supernovae, recombination controls the release of the internal energy generated by strong supernova shocks. For CEEs, however, there is no such supernova-provided energy input. Instead the energy released by recombination itself may dominate the energy budget of many outbursts (6). The unbound mass  $m_{\text{unb}}$  could potentially radiate – simply due to

recombination – as much energy as

$$E_{\text{recom}} \simeq 2.6 \times 10^{46} \text{ ergs } (X + 1.5Y f_{\text{He}}) \frac{m_{\text{unb}}}{M_{\odot}}. \quad (3)$$

Here  $X$  is the mass fraction of hydrogen and  $Y$  is the mass fraction of helium. Hydrogen would initially be ionized in almost all of the likely ejected material from most stars; however helium may be fully ionized only in some fraction of it, denoted  $f_{\text{He}}$ . The role of recombination in a CEE has hitherto been a debated issue in the overall energy balance, the controversy arising from whether it can be effectively converted into mechanical energy to help eject the CE (7–9). This energy budget for the outburst may be increased by the thermal energy of the ejecta. Much of the pre-CEE thermal energy of the ejecta may be expended on adiabatic cooling (6). However, the shock-heating caused by the CEE could well be substantial in some cases.

We now estimate the extent of the parameter space of CEE outbursts, using the model described above to predict the diversity of real events. We assume that  $E_{\text{k}}^{\infty}$  scales with the gravitational potential at the surface of the primary star (2), and use the dimensionless factor  $\zeta$  to write  $E_{\text{k}}^{\infty} = \zeta(Gm_1^2 f_{\text{m}})/R_{\text{init}}$ , where  $f_{\text{m}} = m_{\text{unb}}/m_1$  is the fraction of the total primary mass  $m_1$  that becomes unbound. From equations 1 and 2, this leads to  $L_{\text{P}} \propto (f_{\text{m}}^2 m_1^7 R_{\text{init}}^{-1} \zeta^5)^{1/6}$  and  $t_{\text{P}} \propto (f_{\text{m}}^2 m_1 R_{\text{init}}^2 \zeta^{-1})^{1/6}$ . Two families of events seem likely, one for mergers (i.e.  $f_{\text{m}} \ll 1$ ), and one for CE ejection (i.e.  $f_{\text{m}} \leq 1$ ) (Fig. 1).

In addition to the predicted ranges of outburst energy and duration, this model for CEE outbursts has several noteworthy features. The physics that causes the plateau-shaped light-curve should lead to a difference in the photometrically-inferred expansion velocity and the actual material velocity (which could be inferred from spectra). The effective photospheric temperature should be  $\sim 5000\text{K}$  for thick ejecta (4), and so the outburst color will naturally be red. In addition, once the ejected envelope has fully recombined, the material may suddenly become transparent — unless enough of the ejecta has cooled down sufficiently to produce dust. These characteristics are reminiscent of curious transients with predominantly red spectra recently detected in the local universe (e.g., (10–17)). This empirical class has been dubbed Luminous Red Novae (LRNe), a subset of the even more ambiguously defined class of intermediate luminosity red transients (ILRTs) (2). ILRTs cover a wide range of outburst energies – from  $10^{45}$  to a few  $10^{47}$  ergs (brighter than the brightest novae, but still fainter than Type Ia supernovae). They are characterized by spectroscopically inferred expansion velocities of 200-1000 km/s – much lower than would be expected for novae or supernovae, and also strikingly different from the photometric expansion velocities (18). In addition, some could be seen as red giants within a dozen years after the outburst (16, 19).

It was not known what ILRTs are or whether they have a common cause; several ideas have been suggested (2). A model which considered the possibility that LRNe are caused by stellar mergers – a subset of CEEs – has been independently considered several times

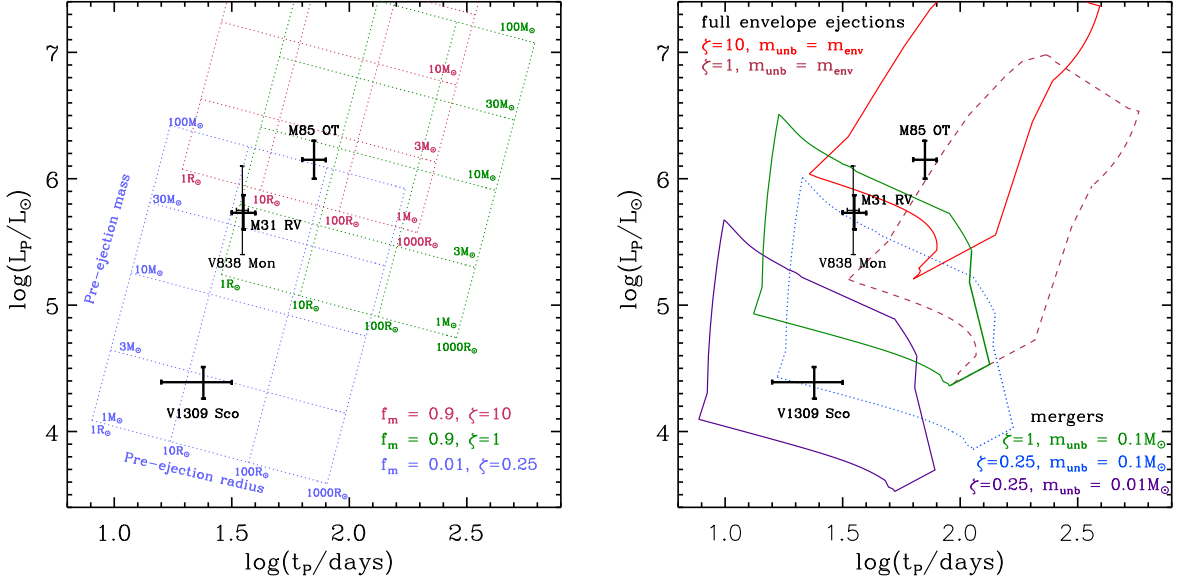


Figure 1: **Left panel:** Model diversity in the  $L_P - t_P$  parameter space is indicated by lines representing constant primary mass and radius.  $f_m$  is fractional mass loss and  $\zeta$  is the kinetic energy at infinity, parametrized as a fraction of the binding energy at the surface of the primary star. Stellar mergers are in a regime of little mass ejection, while  $f_m = 0.9$  approximates full envelope ejection. **Right panel:** Estimated ranges of the plateau luminosity  $L_P$  and duration  $t_P$  for primary stars with ZAMS masses from 1 to 150  $M_\odot$ .  $m_{\text{unb}}$  is the ejecta mass. It is assumed that mergers can happen anytime during the primary's evolution, whereas full envelope ejection can occur only for post-MS primary stars. We used fitting formulae for stellar evolution (24), at  $Z_\odot$ . In both panels, values for  $L_P$  and  $t_P$  are marked for the outbursts from V1309 Sco, M85 OT, M31-RV, and V838 Mon.

for different LRN outbursts, though further examinations of outburst features always showed various drawbacks. However, those problematic features do match expectations from our CEE-driven outburst model (2).

A particular feature of the LRN outbursts – as opposed to all ILRTs – is the presence of a plateau in their luminosity curves. We compare well-known LRNe (2) to the expected CEE diversity in Fig. 1. The agreement is striking, especially given the simplicity of the model and the potential complexities it neglects – e.g., how CEE ejecta deviate from spherical symmetry, or how much  $\zeta$  for mergers might be different to  $\zeta$  for full envelope ejection (2).

M85 OT2006-1 is a LRN with well-known peak luminosity and plateau duration. If the luminosity from M85 OT2006-1 was largely from recombination,  $\sim 1.5M_{\odot}$  of plasma would have recombined to provide the observed total energy. This fits with constraints on the progenitor mass ( $\leq 2M_{\odot}$ ) from the stellar population age (20). Thus M85 OT2006-1 plausibly ejected the whole envelope of a low-mass giant. This outburst showed a plateau, with luminosity  $\approx 1\text{--}2 \times 10^6 L_{\odot}$  (21) for  $\approx 60\text{--}80$  days, and had expansion velocities of 350 km/s (14). Our inferred ejecta mass and that observed expansion velocity indicate a kinetic energy of  $\sim 1.8 \times 10^{48}$  erg. Then  $R_{\text{init}} = 45R_{\odot}$ , self-consistent with our model, gives  $L_P \sim 10^6 L_{\odot}$  and  $t_P \sim 70$  days.

Another recent outburst, V1309 Sco, is similar to, but fainter than, most LRNe, as it radiated away only  $\sim 3 \times 10^{44}$  erg during a  $\sim 25$ -day plateau-shaped maximum in the light-curve (19). The progenitor was a contact binary with a relatively rapidly-decaying orbital period of  $\sim 1.4$  day. After the outburst, the system appeared to be a single star; therefore this appears to have been a CEE, leading to a merger (19). However, several features of the V1309 Sco outburst – in particular the plateau in the light-curve and sudden transparency – were difficult to reconcile with prior theoretical expectations for the appearance of a CEE (2).

Because the V1309 Sco progenitor was observed in detail, this system is ideal for testing our model. Beginning with the properties of the pre-merger contact binary (19, 22), we calculated the amount of material that became unbound during the V1309 merger using two methods – simple energy balance using a 1D stellar code and a set of 3D hydrodynamical simulations (2). Both methods predict that a small mass,  $\sim 0.03$  to  $0.08M_{\odot}$ , will become unbound. Complete recombination of this ejected mass would provide enough energy ( $\geq 7 \times 10^{44}$  ergs) to explain the total energy output of V1309 Sco. The output of the 3D simulations, combined with Equations 1 and 2, predicts plateau durations from 16 to 25 days, and plateau luminosities of  $1.8\text{--}2.2 \times 10^4 L_{\odot}$ . These values match the observed luminosity ( $L_P \sim 2 \times 10^4 L_{\odot}$ ) and plateau duration (about 25 days).

Considering the menagerie of theoretically-expected outbursts from CEEs, we note that events in the top-right of Fig. 1 should be relatively rare [compare with  $\eta$  Car; see (2)], and those in the bottom-left (stellar mergers) comparatively hard to detect in a magnitude-limited survey. Assuming that the peak luminosity of the outburst is about an order of magnitude higher than

$L_P$ , we find that the whole range of  $L_P$  and  $t_P$  for stellar masses  $1 - 150M_\odot$  coincides well with the observed domain for luminosities and durations of LRNe suggested in (23). We can estimate the rate of CEE-originated outbursts that appear as red transients, by considering what fraction of stars in the galaxy undergo a CEE. We estimate 0.024 such events per year per Milky Way-like galaxy (2), of which about half should be more luminous outbursts (results of a CE ejection), and half are lower-luminosity events (powered by stellar mergers). This is consistent with the empirical lower limit for more luminous ILRTs of  $0.019 \text{ yr}^{-1}$  for the Galaxy (20), because we do not expect that all luminous ILRTs must be powered by a CEE [though some non-LRN ILRTs–like NGC 300-OT or SN2008S – might potentially also be triggered by CEEs (2)].

The question of whether recombination energy can help to unbind a stellar envelope during a CEE is important for understanding the formation and survival of many binary systems (8, 9). Our model suggests that a large fraction of the energy from recombination is commonly radiated away following a CEE. Such luminosity provides a beacon, which helps to illuminate and identify a CE ejection or merger at large distances. The recombination wave also controls the shape of the plateau-shaped light-curve of LRNe. We therefore suggest that detecting and characterizing the population of ILRTs will help us understand CEEs.

## Supplementary text

Here we provide additional information about our hydrodynamical simulations, as well as give more details behind our formulae and arguments from the main text.

### S1. Intermediate Luminosity Red Transients

In recent years, observers have identified a new class of transients, with peak luminosities somewhere between that of the brightest novae and Type Ia SNe and with a total energy output anywhere from  $10^{45}$  to a few  $10^{47}$  ergs, e.g., (10–17). Because their spectra are predominantly red, completely unlike novae, they have been called intermediate luminosity red transients (ILRTs, (25)). However alternate names are also in common use, either for all of the transients or for particular kinds of events, e.g. Luminous Red Novae (LRNe), intermediate luminosity optical transients, mid infra-red transients, V838 Mon-like events, and supernova impostors. The relative novelty of these classes, and the uncertainty over their physical origins, makes it unsurprising that the use of such terms is not necessarily always consistent between different papers.

It is not known what red transients are or whether they have a common cause: it has been argued that ILRTs could be due to accretion-powered jets (26), tidal disruption of planets (27), nuclear outbursts (28), electron-capture SNe (29) with shocks propagating through dusty surroundings (30), or violent stellar mergers (31). It has also been argued that – despite having similar outburst properties in terms of color and luminosity – ILRTs may have different origins

(25).

In this work, we consider the particular group of red transients which are most frequently labeled as LRNe. The widely-recognized members of this class of red transients are M31-RV, V838 Mon, and M85 OT2006-1. We note that the recognition of LRNe as a special class of stellar explosion started with the last object in that list, although it was not the first of them to be detected. In this paper we also include V1309 Sco as a possible member of this LRN class, at the low-energy end (19). Another suggested low-energy end LRN is V4332 Sgr – this transient radiated away a total energy of only  $4.5 \times 10^{43}$  ergs (32), an order of magnitude less even than V1309 Sco. The LRN class is likely separated from another class of red transients where progenitors were observationally identified to be dusty modestly-massive stars (with  $M \sim 10M_{\odot}$ ) – as for example in the cases of SN 2008S and NGC 300 OT (18, 33, 34); those ILRTs are better known as supernova impostors. Nonetheless, because the recognition of red transients as a new type of astrophysical object is very recent, their classification is not yet by any means universally established or finally accepted throughout the astrophysics community.

We note that some investigators have suggested that LRNe could be present only in old populations, with V838 Mon standing as an exception (see also the discussion against this point of view in (35)). It is important to clarify that our proposed link between CEEs and LRNe implies that there should not be any such restriction on population age for LRNe: our CEE outburst model is related only to the reason of the ejection – a CEE – and to the self-similar physics and recombination outburst following the CEE. Indeed, CEEs may occur in binary stars with companions of any masses. In terms of rates, CEE from massive stars are expected to be much more rare, as their relative fraction in the total number of stars is small; however they are not forbidden. In addition, given the current understanding of CEE physics, it is impossible to say how the CE ejection would differ in low-mass and high-mass stars.

## **S2. Previous problems with a merger model: what does the standard CEE model predict?**

One of the most common models suggested to explain different LRNe – V838 Mon, M85 OT 2006-1 and V1309 Sco – is a merger, either of two stars, or of a star with a planet (e.g., (13, 19, 31, 39)). It is also known as the merger-burst model; however, because a merger is a particular type of CEE, we will hereafter refer to it as to a CEE model. The case of V1309 Sco is rather unequivocally a CEE, as observations revealed a binary prior the outburst and a single star after (19). However, there were problems with justifying the physics behind this model. For example, a stellar merger scenario in the case of M85 OT2006-1 was rejected because an analysis of the energy available from a merger suggested that a violent merger would be unable, by a factor of a few, to explain the energy that was radiated away from M85 OT2006-1 (20). In (37), striking similarities between the M31-RV, V838 Mon and V4332 Sgr outbursts were

noticed, leading to a discussion which concluded that the merger-powered outburst models proposed to-that-date showed too much dependency on metallicity, mass, and ages and hence could not explain the observed homology.

We list next a number of striking observational features of LRNe which were not previously theoretically anticipated by a CEE model (one leading to either a merger or a the formation of a close binary) and which were not emphasized as discriminating features in previous studies:

- **Large increases in radius and luminosity.** In previously published CE simulations, the increase in the stellar radius of the bound mass during fast spiral-in is usually less than a factor of 10 (see e.g., (40, 41)). These simulations were performed for binaries that are expected to survive, rather than merge, i.e. these binaries have more energy injected into the stellar envelope – relative to the binding energy – than for binaries that merge. However the well-studied example V 1309 Sco reached a maximum luminosity  $\sim 3 \times 10^4 L_{\odot}$ , about  $\sim 5000$  times larger than the initial luminosity of the progenitor ( $\sim 3.0 - 8.6 L_{\odot}$ ), whilst its effective temperature dropped to  $\sim 4000\text{K}$  during the peak luminosity and plateau (19). This indicates an increase in its apparent (or effective) radius by about 90 times, reaching  $\sim 300 R_{\odot}$  (19), at least an order of magnitude more than simulations suggested. Similarly, interferometric observation showed that V838 Mon expanded by  $\sim 300$  times during the outburst, to  $1570 \pm 400 R_{\odot}$ , while its progenitor was likely  $5 - 10 M_{\odot}$  with a radius of only about  $5 R_{\odot}$  (42).
- **An unexpectedly long duration.** Expansion of the envelope during CEE is expected to occur during the dynamical plunge-in phase (see, e.g., (1)), i.e. the stage during which the inspiralling star loses most of its angular momentum. It is theoretically expected, and confirmed by numerical simulations (see e.g. (40, 41)), that this phase proceeds on a timescale of about several *initial* dynamical timescales of the stellar envelope of the primary star. This is a few days for the case of V1309 Sco; however, the outburst lasts  $\approx 100$  days (19), also see Fig. S1) which is comparable to dynamical timescale of this object at the *maximum* of expansion,  $\tau_{\text{dyn,max}} \approx 80$  days. In the case of V838 Mon, the outburst last for about 80 days (43) while the initial dynamical timescale would be only a couple of hours. In case of M85 OT2006-1, in which the outburst last about 60 days (14), there are no strong constraints on progenitor.
- **Plateau phase.** Several ILRTs outbursts, after the initial rise in brightness, featured a plateau in their light curves in the red band at a luminosity somewhat lower than at the maximum. Specifically, in case of V1309 Sco the plateau duration is  $\sim 25$  days (depending on the definition of the start and the end of the plateau phase, from 16 to 31 days (19), also see Fig. S1),  $\sim 60 - 80$  days in case of M85 OT2006-1 (14),  $\sim 15$  days in case of V4332 Sgr (32), although the start of the outburst is not well known) and  $\sim 30 - 40$  days in



case of M31-RV (37). V838 Mon has a very complex visual band light-curve with several peaks separated by about 30 days. Nonetheless, it does have an easily distinguished plateau in the red part of the spectrum as well as in bolometric luminosity; the overall duration of the outburst is about 80 days, and that plateau starts  $\sim 30$  days after the peak luminosity and lasts for another  $\sim 35$  days (36, 44). Most of the energy in LRNe is radiated away during the plateau phase. The plateau shape had not been predicted and had not yet been explained.

- **An extremely rapid decline.** The post-common-envelope decline in luminosity of the merger product is expected to occur on a thermal timescale, which – for these over-luminous and over-inflated objects – is typically about a year. However, the abrupt decline in luminosity (by a factor of 100) in V1309 Sco, M31-RV, V4332 Sgr and V838 Mon happened in a dozen days (19, 32, 36, 37, 44), also see Fig. S1). For V 1309 Sco, the timescale for exponential decrease was determined to be only a few days (19). Strikingly, the timescale for this sharp luminosity decrease is considerably shorter than the dynamical timescale  $\tau_{\text{dyn,max}}$  at the maximum of expansion for V 1309 Sco (80 days) or for V838 Mon (about 500 days).
- **Inconsistent velocities.** While expansion velocities from the spectra were several hundred km/s (e.g., in V1309 Sco (19), in M85 OT2006-1 (14), and in V838Mon (45)), velocities inferred from the apparent radius expansion imply speeds from only about 20 km/s (V 1309 Sco) to about 100 km/s (V838 Mon).

In section S3 below we explain how the model presented in this paper naturally accounts for the above features.

### S3. Wavefront of cooling and recombination in a CEE

As discussed above, the light curves of LRNs have five similar striking features, where two are the most exceptional in providing important clues to the physics of the outburst. First, the outbursts have a roughly constant plateau luminosity  $L_p$  for a time  $t_p$  that is typically dozens of days (for a note on the special case of V838 Mon see, see §S5). Second, the inferred radius of the photosphere increases relatively slowly during most of the plateau phase, at the end of which the apparent radius decreases very quickly. This is reminiscent of the behaviour of type IIP supernovae, in which the photosphere does not stay at a fixed Lagrangian coordinate but moves inwards in mass as the ejecta expands and cools; roughly self-similar, homologous expansion means that the radius of the photosphere and luminosity of the emission remain approximately constant (4, 46–49).

Such a photosphere-defining ‘cooling wave,’ propagating inward in the frame of the expanding shock, was predicted for terrestrial explosions in air by (50, 51). This type of behaviour does not

need to be associated with recombination; it is only dependent on a non-linear temperature dependence of the opacity of the ejecta (see also (52), which argues that the necessary condition is that the effective opacity increases more rapidly than a cubic power of temperature). The low-opacity material outside the photosphere is able to cool by radiation much more effectively than the hot, high-opacity material inside. However, in the case considered here, as well as for type IIP SNe, recombination is the cause of the change in opacity that leads to this cooling-wave. The location of the effective photosphere is controlled by a sudden large reduction in the mean opacity of the ejecta after hydrogen recombination.

Even though the mean opacity greatly drops outside the region of recombination, the photons emitted during recombination will not in general escape directly. Although neutral hydrogen has a much lower Rosseland mean opacity when compared to ionised hydrogen, the relevant line opacity of neutral hydrogen is higher than for the ionised material. So the recombination photons themselves have a short mean free path, and there is no reason to expect strong  $H_\alpha$  line emission, even if photons at other wavelengths are free to escape. Uniformly applying the Rosseland mean opacity in this case would be misleading, and full wavelength-dependent radiative transfer would be necessary to simulate precisely the structure of the cooling wave. Hence situations where the location of the cooling wave is defined by recombination are more complicated than the cases first considered by (50, 51), in particular because there is a release of energy from recombination that is coincident with the change in opacity. However, we consider that the energy input is so close to the photosphere that it justifies neglecting the effect of any heating on the main features of the hydrodynamics.

This physics is well-studied in the context of supernovae, and we can apply appropriate results here. The analytic model of (4), based on the idea of there being a wavefront of cooling and recombination (WCR), is particularly attractive. Although the method produces only approximate light curves, it provides accurate scaling relations that give insight into the underlying physics and to the interpretation of observations. Indeed, (5) verifies the major results of the Popov model with detailed hydrodynamical simulations that include radiative transfer.

The analytic WCR model has the following intrinsic features:

- a) An outburst has a plateau phase. (For more on the condition which must be satisfied in order to obtain a plateau, see below.);
- b) Because the observable surface during the outburst is not the stellar surface, but instead the photosphere of the expanding ejected material defined by the location of the WCR, a large apparent radius increase is expected;
- c) As this recombination front propagates inwards through the material by mass, its geometrical distance to the center can gradually increase and then decrease until the recombination

of the material is over (see Eq. (16) in (4)), while at the same time the outflow passing through the WCR continues to stream outward. This leads to what could be observationally identified as an inconsistency between measured material expansion velocities and apparent expansion of the radiating surface: the photometric velocity indicating the expansion rate of the photosphere can be much less than spectroscopic velocities, which give the speed of the gas passing through the photosphere;

- d) The model connects the outburst not with the dynamical timescale on which the CE rapidly expands, but with the timescale over which recombination wave proceeds;
- e) After the recombination is completed, the model allows sudden transparency, which could be observed as rapid decline of luminosity and appearance of the central object. If material above the front is dense and cool enough, it could form dust that would hide the central object again (for a discussion of dust formation in the ejecta of a related class of transients then see, e.g., (53)).

The recombination process depends strongly on how not only temperature, but also density, evolves. Hydrodynamical simulations show that recombination temperature in this model is  $\sim 5000 - 6000\text{K}$  for thick and dense ejected envelopes, as in case of SNIIP (4,5). Somewhat colder recombination temperatures are expected in less dense ejecta, where the number density of free electrons (which are required for recombination) is smaller. In the grey atmosphere approximation, the effective temperature is a factor of  $2^{1/4} \approx 1.2$  larger than the recombination temperature, corresponding to effective temperatures in the  $\sim 4000 - 6000\text{K}$  range (see also (54) who showed that effective temperatures shift to lower values once the energy of the outburst is decreasing). Although full 3D hydrodynamical simulations with radiative transfer are necessary for more detailed calculations of the effective temperature, it is clear that the WCR model predicts that a CEE outburst will be bright in the red part of the spectrum. The above is a simplification of the complicated situation occurring in these photospheres (e.g. it neglects the role of  $H^-$  ions formed due to electrons donated from metals), but the outcome of a detailed analysis should yield similar conclusions.

For this study, we take the WCR model derived by (4), in the convenient form expressed by (49), and re-scale it to the situation we are studying.<sup>1</sup> We scaled opacities to  $0.32 \text{ cm}^2 \text{ g}^{-1}$  for  $X = 0.7$ . The original derivation by (4) assumed that the kinetic energy input produces self-similar expansion of an envelope moving with constant velocity. This implies that the potential well of the exploding star has already been overcome, and hence that energy input for his equations in the case of CEE is the same quantity as  $E_k^\infty$ .

---

<sup>1</sup>For equation (1) in the main text, we have corrected a small numerical error in the coefficient of equation (9) of (49), for the plateau luminosity, such that it is consistent with the (4) value.

An important assumption in Popov's model is that recombination, although controlling the energy release through its effects on opacity, does not dominate the dynamics of the expansion. In the case of CEE, we can estimate from Eq. (3) of the main paper how much energy is available from recombination. For typical cases of partial envelope ejection, such as in the simulated case of V1309 Sco below, the kinetic energy in the outburst is  $E_k^\infty \sim 3\text{--}4 \times 10^{47} \text{erg} m_{\text{unb}}/M_\odot$ , exceeding the recombination energy by more than an order of magnitude. For cases of complete CE ejection, we can estimate the kinetic energy  $E_k^\infty$  to be of the same order as the initial potential energy of the CEE progenitor-star:  $E_k^\infty = Gm_{\text{unb}}(m_1 - m_{\text{unb}})(\lambda R_{\text{init}})^{-1}$ , where  $\lambda$  is an envelope structure parameter that is roughly of order unity for small low-mass giants but that can be as small as 0.01 for massive and larger giants (55). Then

$$\frac{E_k^\infty}{E_{\text{recomb}}} \sim 150 \times (X + 1.5Y f_{\text{He}})^{-1} \frac{m_1 - m_{\text{unb}}}{M_\odot} \left( \frac{\lambda R_{\text{init}}}{R_\odot} \right)^{-1}.$$

So  $E_k^\infty$  easily exceeds  $E_{\text{recomb}}$  by at least an order of magnitude. Hence, although the recombination energy is a larger fraction of  $E_k^\infty$  in the CEE problem than it is in the Type IIP SNe problem, the recombination energy is still relatively small enough that we feel justified in assuming that it should not play a significant role in driving the dynamics, therefore making Popov's model applicable for CEE.

We briefly clarify here that the analysis for  $E_k^\infty$  above must self-consistently extend to the choice of  $\zeta$  for complete envelope ejection. For that reason, a typical  $\zeta$  for complete envelope ejection might be expected to be somewhat higher than a typical  $\zeta$  for ejection resulting from a merger event. In those extreme cases where  $\lambda = 0.01$  then an assumption of  $\zeta = 100$  would become reasonable, though the range  $1 < \zeta < 10$  seems likely to be more typical.

In Popov's simplified analytical model for the WCR, the main role of recombination is to provide the reason that the gas switches from opaque to transparent, resulting in a plateau-shaped light-curve. The Popov model predicts that light curves will be self-similar to each other, with their shape characterized by the dimensionless parameter  $\Lambda$ : larger values of  $\Lambda$  correspond to more pronounced plateaus. We find that, scaling for the case of CEE-outbursts,  $\Lambda$  from (4) can be calculated as

$$\Lambda \approx 49 \left( \frac{R_{\text{init}}}{3.5R_\odot} \right)^{-1} \left( \frac{E_k^\infty}{10^{46} \text{erg}} \right)^{-1/2} \left( \frac{m_{\text{unb}}}{0.03M_\odot} \right)^{3/2} \left( \frac{\kappa}{0.32 \text{cm}^2 \text{g}^{-1}} \right)^2 \left( \frac{T_{\text{rec}}}{4500 \text{K}} \right)^4,$$

which for cases of complete envelope ejection becomes

$$\Lambda \approx 1700 \lambda^{1/2} \left( \frac{R_{\text{init}}}{R_\odot} \right)^{-1/2} \left( \frac{m_{\text{unb}}^2}{(m_1 - m_{\text{unb}})M_\odot} \right)^{1/2} \left( \frac{\kappa}{0.32 \text{cm}^2 \text{g}^{-1}} \right)^2 \left( \frac{T_{\text{rec}}}{4500 \text{K}} \right)^4.$$

Consequently, for most of the range of possible CEE-progenitors,  $\Lambda \gg 1$ , and hence a plateau phase with sudden transparency is predicted. If  $\Lambda \ll 1$ , which is not a likely case for

CE progenitors, the model predicts slow decline with no well defined plateau in the light-curve. Cases with intermediate values of  $\Lambda \sim 1$  may provide a phase somewhat like a plateau, with the luminosity taking a comparatively long time to decline after recombination is completed (see also Fig. S2).

We note that these scaling relations were derived under the approximation that the ejection is spherically symmetric, which may well be less accurate here than for supernovae. In addition, (4) assumed that the plasma was radiation dominated, which may well be less appropriate for matter ejected from a stellar merger than for supernova ejecta. However, it has previously been noted that at the location of the cooling wave recombination itself will automatically lead to radiation becoming dominant (e.g., (3)), which helps to justify our adoption of the Popov expressions. Indeed, (6) show that during the recombination phase the third generalized adiabatic index ( $\Gamma_3$ ) decreases below the normal value for radiation-pressure dominated matter, even for initially gas-pressure dominated matter. This allows continued expansion by an order of magnitude or more at near-constant temperature – independent of whether the initial matter is gas- or radiation-pressure dominated – and also increases the relative importance of radiation pressure, even in initially cold envelopes.

#### S4. Simulations of V1309 Sco

For the properties of the pre-merger contact binary in V1309 Sco, we take a low-mass subgiant with mass  $M_1 \sim 1.52M_\odot$  and radius  $R_1 = 3.5R_\odot$  with a lower-mass companion of  $M_2 \sim 0.16M_\odot$  (22), with an orbital period at Roche Lobe overflow of  $P_{\text{orb}} \sim 1.42$  days (the last detected orbital period before the merger, (19)).

The binding energy of the envelope of a subgiant representing V1309 Sco primary is  $|E_{\text{bind}}| \simeq 1.5 \times 10^{48}$  ergs (as is standard, here we include both the gravitational potential and internal thermal energy terms but not the recombination term). Stellar model calculations were performed using the `STARS/ev` stellar evolution code, originally developed by Eggleton (56–59), with recent updates described in (60, 61) and references therein. For this companion mass of  $0.16M_\odot$ , even if the companion survives the entire spiral-in and the orbital energy is released as close as possible to the boundary of the primary’s core (i.e. providing the maximum possible energy output), the merger would produce only about  $\Delta E_{\text{orb}} \simeq 5 \times 10^{47}$  erg. This is only a third of the envelope’s binding energy. So a CEE in this system necessarily results in a merger before the envelope is unbound.

However, for this particular primary, soon after the companion starts to plunge-in, the released orbital energy near the surface exceeds the binding energy of that part of envelope already outside the location of the companion. From the detailed stellar model, we find that the mass that can become unbound during this initial phase of the spiral-in is  $m_{\text{unb}} \approx 0.04M_\odot$ . The total orbital energy that was deposited in this mass is  $\sim 6 \times 10^{46}$  ergs; some of this material will

be ejected only barely faster than the local escape velocity ( $v_{\text{esc}} \approx 420 \text{ km/s}$  for the unperturbed star) and some will get significantly more specific kinetic energy. Ejected matter that is given more energy than is required for overcoming the potential barrier will still have non-zero kinetic energy at infinity  $E_k^\infty > 0$ ; this will be smaller than the total energy deposited, but should be of the same order.

The magnitude of the initial velocity  $v$  of the ejected upper layers can be qualitatively understood by considering a circular binary consisting of two companions with masses  $m_1$  and  $m_2$ , orbital separation  $a$ , and total orbital angular momentum  $J$  approximated by Keplerian two-body expressions:  $J = \mu \Omega a^2 = m_1 m_2 (Ga/M)^{1/2}$ , where the reduced mass  $\mu = m_1 m_2 / M$ ,  $\Omega^2 = GM/a^3$ , and  $M = m_1 + m_2$ . To shrink the orbit by  $da$ , a fraction of the orbital angular momentum  $dJ$  must be transferred to a portion  $dm_1$  of the stellar envelope material. This angular momentum transfer occurs in the very top layers of the primary star, and hence the stellar mass which is inside the orbit of the companion star does not significantly change. Therefore, treating  $m_1$  and  $m_2$  as constant,

$$dJ \approx \frac{1}{2} \frac{J}{a} da = \frac{1}{2} \mu \Omega a da .$$

When the companion already orbits inside the envelope,  $a \approx r_1$  (although the  $r_1$  describing particular particles of matter can be somewhat larger than their initial  $r_1$  in an unperturbed star). In the process, the stellar material  $dm_1$  achieves an angular momentum  $dJ = v r_1 dm_1$ , implying a tangential velocity

$$v \approx \frac{1}{a} \frac{dJ}{dm_1} \approx \frac{1}{2} \mu \Omega \left( \frac{dm_1}{dr_1} \right)^{-1} .$$

For the masses and initial orbital period used in our V1309 Sco simulations, we find that this initial tangential velocity is

$$v \approx 2.5 \text{ km s}^{-1} \left( \frac{dm_1/M_\odot}{dr_1/R_\odot} \right)^{-1} .$$

From the mass profile of the larger star's envelope,  $dm_1/dr_1 = 4\pi r_1^2 \rho(r_1)$ , where  $\rho(r_1)$  is the density profile and  $r_1$  is the distance to the center of the donor. In the upper  $0.02 M_\odot$  of our pre-merger  $1.52 M_\odot$  star  $(dm_1/M_\odot)/(dr_1/R_\odot) \sim 10^{-4} - 10^{-1}$ , with smaller values closer to the surface. We note that when mass ejection begins, the layers will expand and somewhat more mass will have even smaller values of  $(dm_1/M_\odot)/(dr_1/R_\odot)$ . A significant fraction of this upper envelope therefore is expected to be ejected at velocities higher than  $v_{\text{esc}}$ . Considering the pre-merger orbital configuration, the expected kinetic energy at infinity is of order  $\sim 10^{46}$  ergs.

The estimates above were made for a symmetric, non-rotating 1D stellar model. For a real – 3D – star filling its Roche lobe, most of the companion-envelope interactions occur close to the orbital plane. There the star's radius would be larger than for 1D models, so we expect that

more mass could be lost in the rotating case. Yet, since most of this expansion of the stellar structure happens in the very outer layers, we do not expect the enhancement to be more than a factor of a few.

From the stellar model, we also find that  $f_{\text{He}} \approx 0.8$ . Hence, if all mass that could become unbound would also recombine, the total energy that can be radiated away during the recombination in V1309 Sco case is  $\sim 10^{45}$  ergs – so the available recombination energy reservoir can explain the observed outburst’s energy very well.

For a better estimate about how much mass could be ejected, we performed several numerical simulations using the 3D SPH code `StarCrash` (62, 63). This code was specifically re-developed to deal with close binary systems (64). For these numerical studies, we varied the initial orbital period around the observed pre-merger value  $P_{\text{orb}} \sim 1.42$  day (19). Table S1 gives the complete list of initial conditions, including rotational synchronization of the giant. The companion was modelled as either a low-mass main sequence star (with SPH particles) or as a point mass (representing the core of a red giant which lost its envelope in a previous binary interaction (22)). Stellar structures were first calculated using the `STARS/ev` code and then relaxed in `StarCrash` in a binary configuration close to Roche-lobe overflow. As a result of this relaxation, the radius of the giant in the orbital plane was slightly larger than its 1D radius obtained with the stellar code, as expected (65).

A visualization of simulation ps334 presents the evolution of the column density (in  $\text{g}/\text{cm}^2$ ) as viewed from a direction perpendicular to the orbital plane (see Movie S1). After the merger,  $\sim 0.06M_{\odot}$  of unbound material is left streaming from the merger product with some deviation from axisymmetry, including clumpiness. In all simulations the merger ejects a small fraction of the donor, and the unbound mass is comparable with our preliminary estimates,  $\sim 0.04M_{\odot}$  (depending on the degree of corotation, it varies from  $\sim 0.03$  to  $0.08M_{\odot}$ , see Table S1). This mass is obtained by computing the total energy (kinetic, gravitational and internal) for each particle: if this energy is positive, the particle is considered to be unbound. We find that for the same donors, having a MS companion will result in less mass ejection. For most simulations, the mass is ejected in two episodes (see Fig. S1), where during the first episode the companion is still outside the giant, and during the second it is plunging-in. In simulations mn351 and ms376, three episodes of mass ejection were observed. In one simulation, ms372, the mass ejection was mostly continuous. The mass ratio between first and second mass ejection varies from about 80% of all unbound mass being ejected during the first mass outburst to about 36%. The time interval between the starts of the first and last mass outbursts varies from 1 to 9 days, and the specific kinetic energy during the first mass outbursts is larger (see, e.g., Fig S3).

As reported in Table S1, the kinetic energy of the unbound material at infinity  $E_{\text{k}}^{\infty}$  is  $\sim 10^{46}$  ergs. The initial energy powering the ejection  $E_{\text{k}}$  is larger, and is partly spent on overcoming the potential well just near the merged star, so  $E_{\text{k}}^{\infty}$  is not identical to  $E_{\text{k}}$ . In each individual

simulation,  $E_k^\infty$  asymptotically approaches some value soon after the merger (see Fig. S3). We find that the total value of  $E_k^\infty$  is larger when the unbound mass is larger, but the specific kinetic energy is lower.

We note that the observed V1309 Sco light-curve (see Fig. S1) might well be reproduced best assuming that, as in most simulations, there were two or three episodes of mass ejection, where in the first episode the unbound mass had higher ejection velocity (Fig S4). It is tempting to interpret this as a promising sign for this model, and not just to the extent that adding more free parameters will always allow a better fit. Nonetheless, we recognise that a strong conclusion with regard to this point requires more sophisticated radiative transfer calculations in order to produce light-curves that properly take into account the asymmetry and structure of the ejected matter. For the case of ps334, the asymmetry of the photospheric surface can be seen in Movie S2.

## **S5. Individual objects**

### **V838 Mon**

V838Mon's light curve is an exception as being more irregular – its V magnitude exhibits three phases of brightening (44), with plateaus being very pronounced in bolometric luminosity (which is dominated by red spectra) during the last two peaks in V. This complex behavior might easily be linked to a dramatic and asymmetric start of a CEE. One way a CEE event can start is because of the Darwin instability (which is likely the case for V1309 Sco, as it is a system presumably with a large mass ratio); in this case a CE is formed almost immediately, on a dynamical timescale. The other trigger for a CEE event is when one of the stars starts overfilling its Roche lobe due to evolutionary expansion (this might be the case for V838 Mon). In the latter case, the creation of a CE does not necessarily occur on a dynamical timescale: at the very beginning of the contact, loss of surface layers is not expected to occur smoothly and continuously. Mass transfer can bring a giant out of contact, either due to a binary expansion or due to contraction of the giant in response to sudden mass loss, and the mass transfer unavoidably will be continued later. This stage of evolution – the start of the CEE in giants – is not well understood and is currently under debate (for a review on the current understanding see (1)). The binary may then proceed to a CEE on a timescale which can be estimated to be anywhere from a year to hundreds of years (1, 66). We suggest hence that the observed three peaks of brightening are most likely linked to either one highly asymmetric interaction resulting in many clumps or to several mass outbursts, similar to the case V1309 Sco discussed above, but possibly not resulting in a merger.

It is remarkable as well that it is likely that V838 Mon is a binary star now (67), and hence may deliver several more interesting eruptive events before it completes its CEE evolution with either merger or the formation of a compact binary.



### **ILRTs from massive dusty stars**

Some red transients have progenitors well identified to be cool red giants surrounded by dust. Noticeable examples are SN 2008S and NGC 300 OT (18, 33, 34). A very good model explaining the physics of an explosion propagating through a cool expanded envelope was developed by (30). A CEE outburst model as described in our manuscript might seem – at first sight – not applicable. To start with, CEE outbursts presume that an envelope is still hot enough to be ionized.

However, the reason for the explosion in that model (30) is not fully established. It has been argued that it could be an electron-capture supernova (18) which occurred in an extreme asymptotic giant branch (AGB) star. The progenitor is suggested to have been a cold star with  $T_{\text{eff}} = 2500\text{K}$  and  $\lg_{10}(L/L_{\odot}) = 4.6$  and  $4.9$ , where the total energies radiated away in the transient stages were  $3 \times 10^{47}$  and  $8 \times 10^{47}$  erg, for SN 2008S and NGC 300-OT respectively (30).

Whilst a progenitor with those properties is consistent with being a massive AGB star, similar characteristics could also be possessed by a red giant during a long-term quasi-stable CEE phase known as the self-regulating spiral-in. This situation is expected to occur if the envelope was not ejected promptly during the plunge-in phase; in this case the companion orbits inside the CE in a very rarefied region and the phase can last hundreds of years (66). The stars appear to be puffed-up and somewhat cooler than would be predicted by standard evolutionary tracks (68). In addition, the initial mass outburst during the initial interaction and the plunge-in (see the discussion on V838 Mon above) will cool down, potentially forming dust around the system. In this case, the main orbital energy release occurs deep inside the star, at the bottom of the expanded envelope. For stars orbiting AGB cores, the orbital energy release can easily be as high as a few times  $10^{48}$  ergs.

We therefore note that we can not rule out CEE from the list of possible triggers of the explosion underlying this subclass of ILRTs, even though the physics of the outburst is different from the WCR-determined model, since the outer parts of the extended envelope are cool enough to have recombined before the outburst.

### **$\eta$ Carinae**

The Great Eruption of  $\eta$  Carinae, which may also have been triggered by a stellar merger (see, e.g., (69) and references therein), was recently measured via light echoes, and was surprisingly cool (70), as would have been produced if a recombination wave defined the photosphere. The amount of energy radiated was certainly too large to have been powered purely by the recombination of a sensible amount of material, so additional energy input would have been required.

## S6. Rates

A lower limit for the ILRT rate from observations is  $0.019 \text{ yr}^{-1} L_{\text{MW}}^{-1}$  (20), where  $L_{\text{MW}}$  represents the luminosity of our Galaxy. With a star formation rate of  $\approx 2M_{\odot}$  per year (though rates can be from 1 to  $10 M_{\odot}$  per year, (71)) and with initial mass function from (72), we find that, per year, roughly 0.3 stars are formed with masses large enough ( $\geq 1M_{\odot}$ ) to evolve off the MS in less than a Hubble time. Roughly half of stars are in binaries, and, for these initial masses, 16% of those binaries evolve via CEE (with 48% of the binaries surviving the CEE and the other 52% experiencing a merger) (73). Hence the theoretically expected rate of CEEs is  $\sim 0.024 \text{ yr}^{-1} L_{\text{MW}}^{-1}$ , in agreement with the observed lower limit.

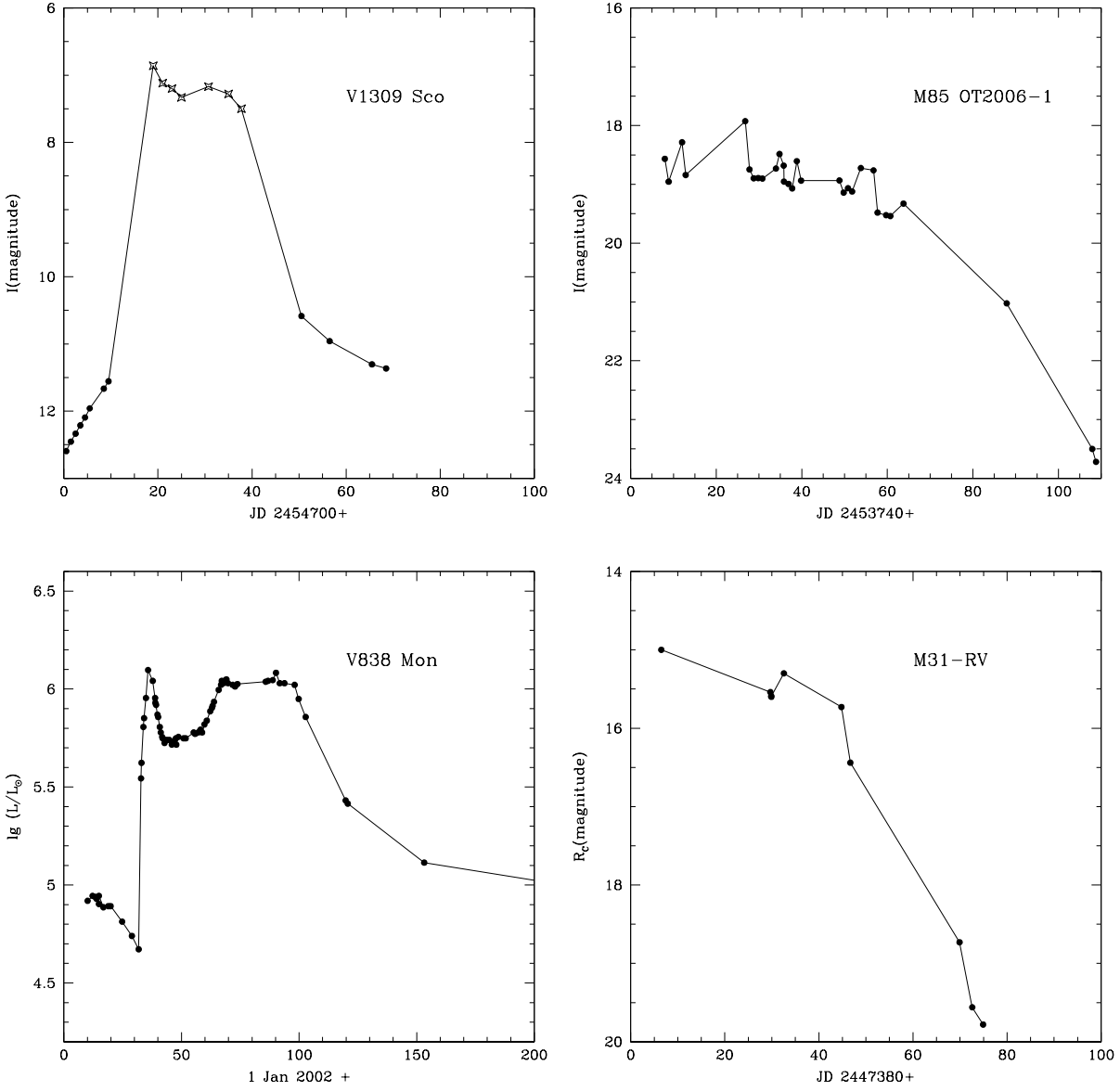


**Fig. S1.** Observed evolution of magnitudes or luminosity for LRNe discussed in the text. Data was taken from (14) for M85 OT2006-1, from (36) for V838 Mon and from (37) for M31-RV. For V1309 Sco, we used data from AAVSVO (available at <http://www.aavso.org/>), marked by asterisk symbols, and from OGLE-II (38), marked as solid dots.

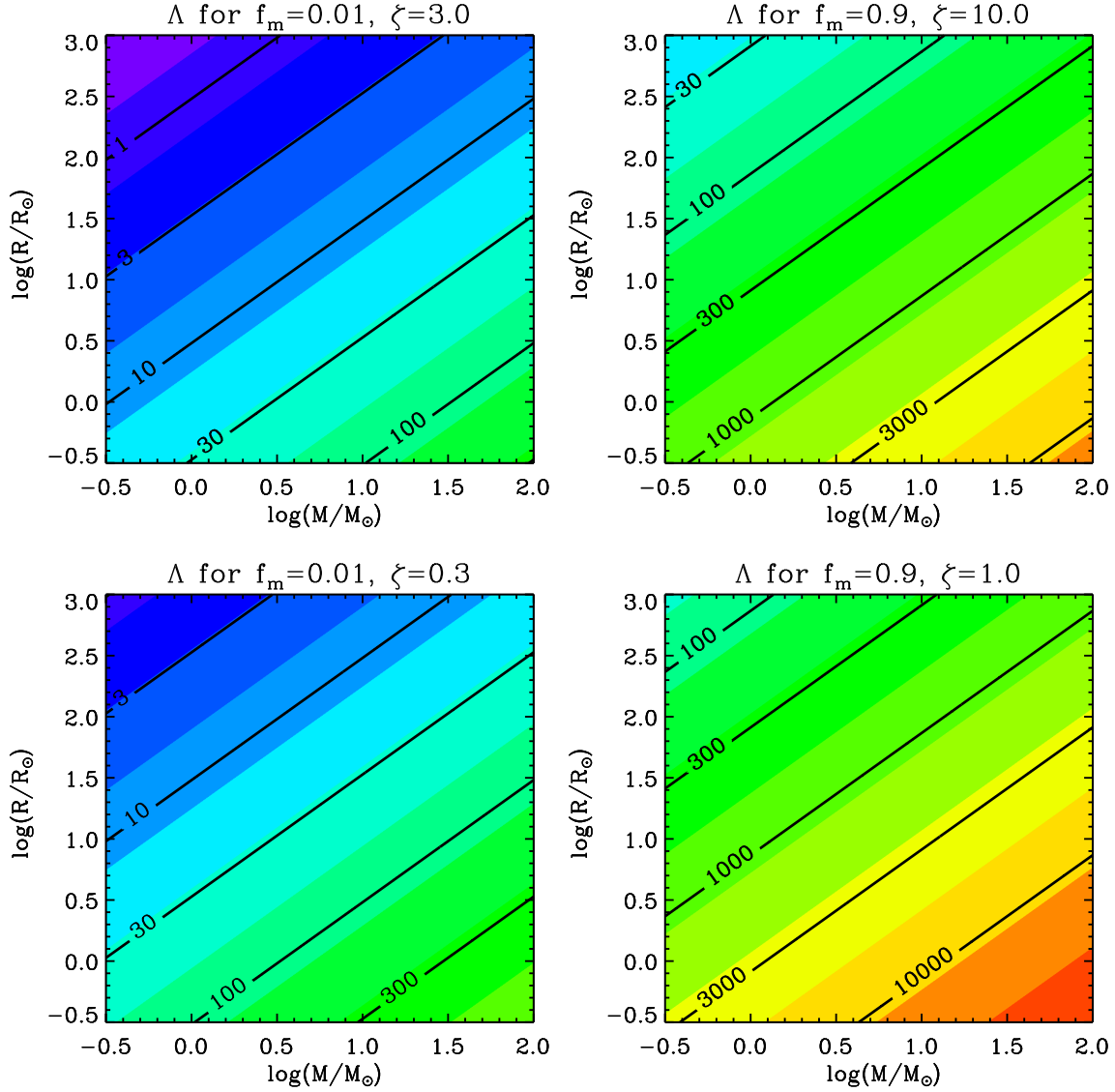


**Fig S2.** Values of  $\Lambda$ , i.e. the parameter which indicates whether the outburst is expected to lead to a plateau, as calculated from (4). We show how these  $\Lambda$ -values vary across a notional pre-CEE mass-radius plane for a selection of parameter choices indicative of different potential physical situations. The two left-hand panels are estimates for mergers which eject one percent of the mass of the primary star (i.e.  $f_m = 0.01$ ); the lower panel adopts  $\zeta = 0.3$  and the upper panel  $\zeta = 3$ . The two right-hand panels represent estimates for envelope ejection (i.e.  $f_m = 0.9$ ); the lower panel adopts  $\zeta = 1$ , and the upper panel  $\zeta = 10$  (as discussed in the text, it is reasonable to expect that  $\zeta$  may typically be higher for full envelope ejection than for mergers). Only when small amounts of matter are lost from unusually large low-mass stars does  $\Lambda$  fall as low as 1. Hence we expect a plateau to be produced in the vast majority of CEE-related outburst light-curves.

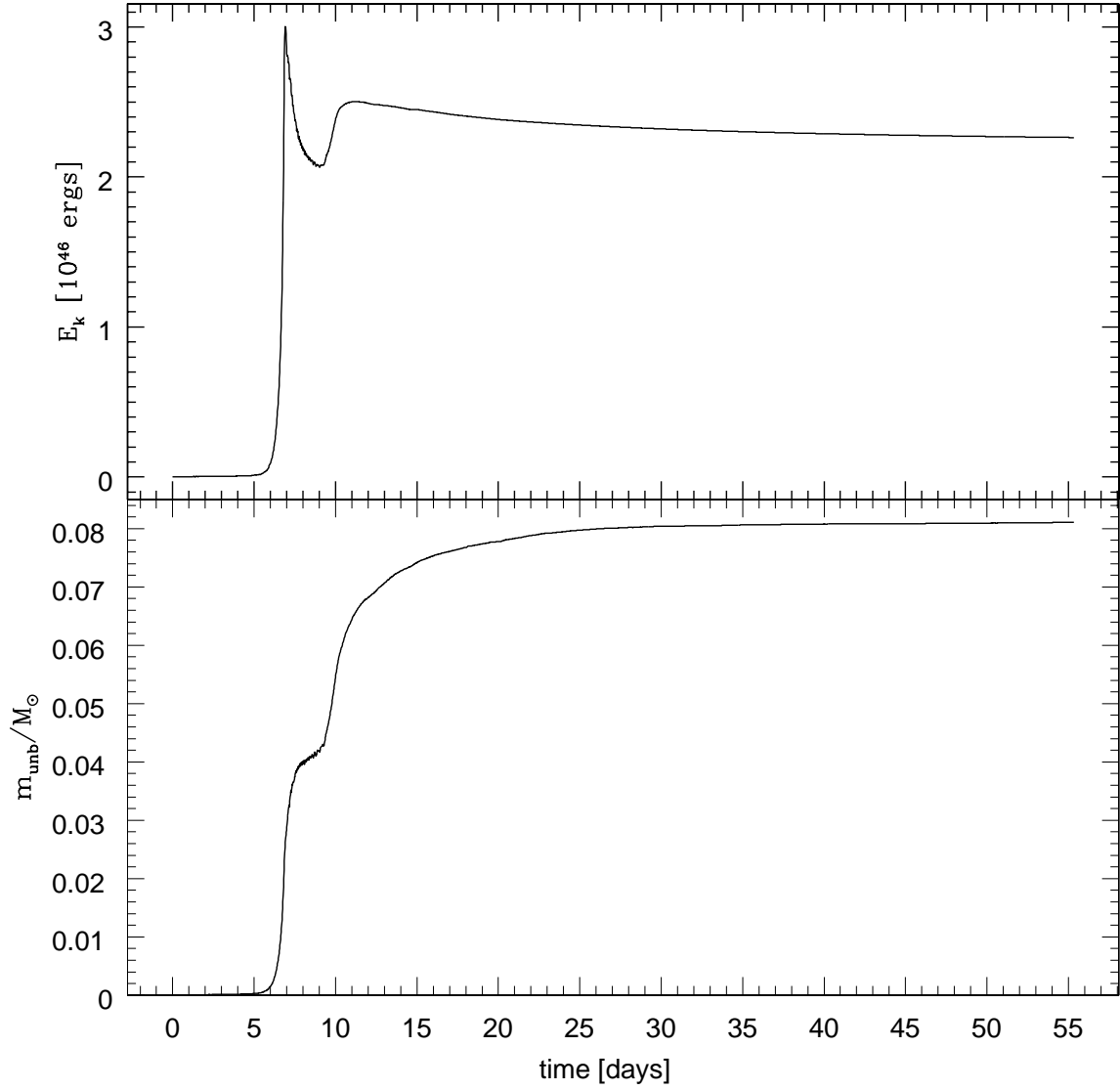


**Fig. S3.** The time evolution of the kinetic energy  $E_k$  of the ejected material (top panel) and unbound mass  $m_{\text{unb}}$  (bottom panel) in simulation ps379. In the lower panel, note the two episodes of mass ejection, near times of 6 days and 10 days.

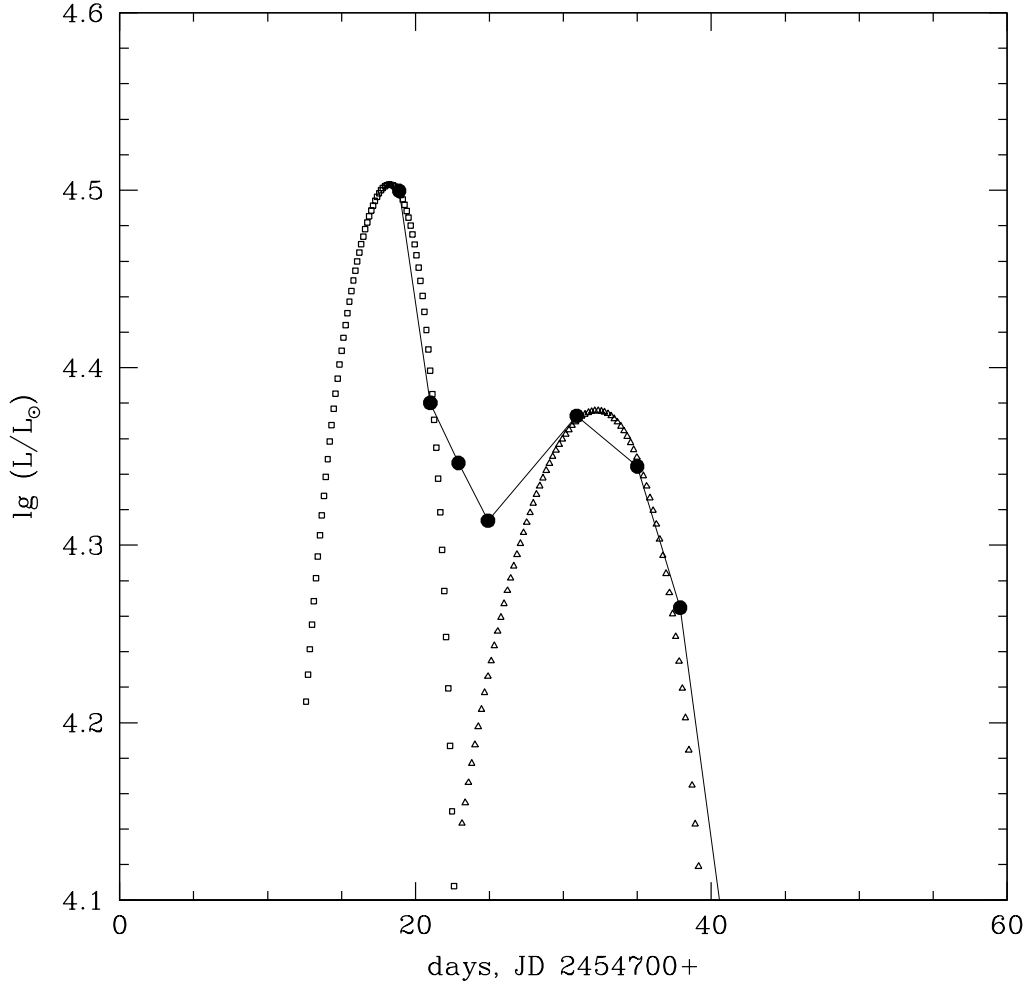


**Fig. S4.** The observed evolution of bolometric luminosity during the V1309 Sco outburst (19) is represented by solid circles and a thin line. We compare this to the solutions of equations (17) and (21) of (4), using two consecutive mass outbursts. The light-curve resulting from the first mass ejection is shown by squares:  $m_{\text{unb}} = 0.02M_{\odot}$ ,  $E_k = 0.9 \times 10^{46}$  ergs,  $E_{\text{TH}}^0 = 0.13 \times 10^{46}$  is the initial thermal energy in this ejected layer,  $E_{\text{th}} = E_k/2 + E_{\text{TH}}^0$  (the material is shocked, the standard case for Popov’s model when  $E_{\text{TH}}^0 \ll E_k$ ), the fit was done with  $T_{\text{rec}}=5000$  K, characteristic for this peak (19). The light-curve resulting from the second mass ejection is shown with triangles  $m_{\text{unb}} = 0.04M_{\odot}$ ,  $E_k = 0.9 \times 10^{46}$  ergs,  $E_{\text{TH}}^0 = 0.75 \times 10^{46}$  is the initial thermal energy in this ejected layer,  $E_{\text{th}} = E_{\text{TH}}^0$  (no shock heating in second ejection. We adopted this for two reasons: a) this layer possesses  $E_{\text{TH}}^0$  larger than it would be suggested by Popov’s approximation  $E_k/2$ ; b) the second mass outburst occurs after the companion is below the ejected layer), the fit used  $T_{\text{rec}}=4000$  K, characteristic for this peak (19). The interval between the beginnings of the two outbursts is 6.7 days.

| Model | $R_1^{\text{ev}}$ | $R_1$ | $a$  | $P_{\text{orb}}$ | $f_{\text{sync}}$ | $f_{\text{RLOF}}$ | $N_{\text{part}}$ | Type | $m_{\text{unb}}$ | $E_k^\infty$ | $L_P$ | $t_P$ |
|-------|-------------------|-------|------|------------------|-------------------|-------------------|-------------------|------|------------------|--------------|-------|-------|
| ps334 | 3.4               | 3.34  | 6.32 | 1.42             | 0.915             | 0.921             | 50000             | PM   | 0.042            | 2.03         | 2.2e4 | 21    |
| mn351 | 3.4               | 3.51  | 6.32 | 1.42             | 0.000             | 0.968             | 100000            | MS   | 0.039            | 1.64         | 2.3e4 | 16    |
| pn351 | 3.4               | 3.51  | 6.32 | 1.42             | 0.000             | 0.968             | 100000            | PM   | 0.061            | 1.63         | 1.8e4 | 22    |
| ps351 | 3.4               | 3.51  | 6.32 | 1.42             | 1.000             | 0.968             | 170000            | PM   | 0.065            | 2.22         | 2.2e4 | 22    |
| ms376 | 3.65              | 3.76  | 6.55 | 1.50             | 1.000             | 0.999             | 100000            | MS   | 0.040            | 1.42         | 2.0e4 | 18    |
| ps376 | 3.65              | 3.76  | 6.55 | 1.50             | 1.000             | 0.999             | 100000            | PM   | 0.056            | 1.87         | 2.1e4 | 21    |
| ms372 | 3.7               | 3.72  | 6.40 | 1.45             | 0.937             | 1.013             | 50000             | MS   | 0.041            | 1.51         | 2.1e4 | 19    |
| ps379 | 3.73              | 3.79  | 6.32 | 1.42             | 0.854             | 1.045             | 100000            | PM   | 0.081            | 2.25         | 2.0e4 | 25    |

**Table S1.** Results from SPH simulations.  $R_1^{\text{ev}}$  is the radius of the donor from the stellar code in  $R_\odot$ ,  $R_1$  is the largest spatial size of the pre-CEE donor in the SPH simulation after relaxation in  $R_\odot$ ,  $a$  is the initial orbital separation in  $R_\odot$ ,  $P_{\text{orb}}$  is the initial orbital period (in days) of the relaxed binary in the SPH code,  $f_{\text{sync}}$  gives the synchronization of the red giant with the orbit (0 is for no rotation, 1 is for fully synchronized),  $N_{\text{part}}$  is the number of particles representing the giant star, and  $f_{\text{RLOF}}$  is the fraction of the radius of the primary with respect to its Roche lobe radius. MS is a main sequence star represented with 20 000 particles in mn351, and with 2000 particles in ms372 and ms376. PM is a point mass. The remaining columns give results and derived quantities:  $m_{\text{unb}}$  is the unbound mass in  $M_\odot$ ;  $E_k^\infty$  is the kinetic energy at infinity in  $10^{46}$  ergs;  $L_P$  is the plateau luminosity in  $L_\odot$  calculated from equation (1) of the main text; and  $t_P$  is the duration of plateau phase in days, calculated from equation (2) of the main text.

**Movie S1.** Column densities in simulation ps334, as viewed perpendicular to the orbital plane and at times after the merger. The merger causes an outflow of material, with the field of ejecta dropping to lower and lower densities and column densities as it expands. At late times in the simulation, while the ejecta continues streaming outward, the bound merger product in the center of the system gradually reaches larger column densities as more material falls back to its surface. Visualizations generated using SPLASH (74).

**Movie S2.** Temperature cross section in the orbital plane. Like visualization S1, the scenario depicted is for simulation ps334, again viewed perpendicular to the orbital plane at times after the merger. Only temperatures between 4000 K and 5000 K are shown, corresponding roughly to the recombination temperature and hence roughly to the location of the photosphere. Note that between  $\sim 165$  and 185 days, lines of sight from an observer looking along the orbital plane do not fully penetrate down to the innermost closed 4500K surface: this enlarged photosphere is the main cause of the a plateau phase. Near  $\sim 185$  days, the shroud dissipates and the inner bound merger product would be revealed, corresponding to the decline stage after the plateau. Visualizations generated using SPLASH (74).



## References and Notes

1. N. Ivanova, *ASP Conference Series* **447**, 91 (2011)
2. Materials, methods are available as supplementary materials on Science Online .
3. N. N. Chugai, *Soviet Astronomy Letters* **17**, 210 (1991).
4. D. V. Popov, *ApJ* **414**, 712 (1993).
5. D. Kasen, S. E. Woosley, *ApJ* **703**, 2205 (2009).
6. D. Kasen, E. Ramirez-Ruiz, *ApJ* **714**, 155 (2010).
7. I. Iben, Jr., M. Livio, *PASP* **105**, 1373 (1993).
8. Z. Han, P. Podsiadlowski, P. P. Eggleton, *MNRAS* **270**, 121 (1994).
9. R. F. Webbink (2008), vol. 352 of *ASSL*, p. 233.
10. J. Mould, *et al.*, *ApJL* **353**, L35 (1990).
11. P. Martini, *et al.*, *AJ* **118**, 1034 (1999).
12. H. E. Bond, *et al.*, *Nature* **422**, 405 (2003).
13. S. R. Kulkarni, *et al.*, *Nature* **447**, 458 (2007).
14. A. Pastorello, *et al.*, *Nature* **449** (2007).
15. H. E. Bond, *et al.*, *ApJL* **695**, L154 (2009).
16. H. E. Bond, *ApJ* **737**, 17 (2011).
17. M. M. Kasliwal, *et al.*, *ApJ* **730**, 134 (2011).
18. E. Berger, *et al.*, *ApJ* **699**, 1850 (2009).
19. R. Tytenda, *et al.*, *A&A* **528**, A114 (2011).
20. E. O. Ofek, *et al.*, *ApJ* **674**, 447 (2008).
21. A. Rau, S. R. Kulkarni, E. O. Ofek, L. Yan, *ApJ* **659**, 1536 (2007).
22. K. Stępień, *A&A* **531**, A18 (2011).
23. A. Rau, *et al.*, *PASP* **121**, 1334 (2009).

24. J. R. Hurley, O. R. Pols, C. A. Tout, *MNRAS* **315**, 543 (2000).
25. H. E. Bond, *et al.*, *American Astronomical Society Meeting Abstracts* (2012), vol. 219 of *American Astronomical Society Meeting Abstracts*, p. 436.09.
26. N. Soker, A. Kashi, *ApJ* **746**, 100 (2012).
27. E. Bear, A. Kashi, N. Soker, *MNRAS* **416**, 1965 (2011).
28. I. Iben, Jr., A. V. Tutukov, *ApJ* **389**, 369 (1992).
29. T. A. Thompson, *et al.*, *ApJ* **705**, 1364 (2009).
30. C. S. Kochanek, *ApJ* **741**, 37 (2011).
31. N. Soker, R. Tylenda, *MNRAS* **373**, 733 (2006).
32. R. Tylenda, L. A. Crause, S. K. Górny, M. R. Schmidt, *A&A* **439**, 651 (2005).
33. J. L. Prieto, *et al.*, *ApJL* **681**, L9 (2008).
34. N. Smith, *et al.*, *ApJL* **697**, L49 (2009).
35. M. H. Siegel, H. E. Bond, *The Nature of V838 Mon and its Light Echo*, R. L. M. Corradi, U. Munari, eds. (2007), vol. 363 of *Astronomical Society of the Pacific Conference Series*, p. 189.
36. R. Tylenda, *A&A* **436**, 1009 (2005).
37. F. Boschi, U. Munari, *A&A* **418**, 869 (2004).
38. A. Udalski, *Acta Astronomica* **53**, 291 (2003).
39. N. Soker, R. Tylenda, *ApJL* **582**, L105 (2003).
40. J.-C. Passy, *et al.*, *ApJ* **744**, 52 (2012).
41. P. M. Ricker, R. E. Taam, *ApJ* **746**, 74 (2012).
42. R. Tylenda, N. Soker, R. Szczerba, *A&A* **441**, 1099 (2005).
43. Crause, L. A., Lawson, W. A., Kilkenney, D., *et al.* 2003, *MNRAS*, 341, 785
44. A. Retter, A. Marom, *MNRAS* **345**, L25 (2003).
45. J. P. Wisniewski, *et al.*, *ApJ* **588**, 486 (2003).

46. V. S. Imshennik, D. K. Nadyozhin, *Soviet Ast.* **8**, 664 (1965).
47. E. K. Grassberg, V. S. Imshennik, D. K. Nadyozhin, *APSS* **10**, 28 (1971).
48. E. K. Grassberg, D. K. Nadyozhin, *APSS* **44**, 409 (1976).
49. R. G. Eastman, S. E. Woosley, T. A. Weaver, P. A. Pinto, *ApJ* **430**, 300 (1994).
50. Y. B. Zel'Dovich, A. Kompaneets, Y. P. Raizer, *JETP* **7**, 882 (1958).
51. Y. B. Zel'Dovich, A. Kompaneets, Y. P. Raizer, *JETP* **7**, 1001 (1958).
52. H. Bethe, *Los Alamos Report LA-3064*, 44 (1964).
53. C. S. Kochanek, D. M. Szczygieł, K. Z. Stanek, *ApJ* **758**, 142 (2012).
54. I. Y. Litvinova, D. K. Nadezhin, *Soviet Astronomy Letters* **11**, 145 (1985).
55. A. J. Loveridge, M. V. van der Sluys, V. Kalogera, *ApJ* **743**, 49 (2011).
56. P. P. Eggleton, *MNRAS* **151**, 351 (1971).
57. P. P. Eggleton, *MNRAS* **156**, 361 (1972).
58. P. P. Eggleton, *MNRAS* **163**, 279 (1973).
59. P. P. Eggleton, J. Faulkner, B. P. Flannery, *A&A* **23**, 325 (1973).
60. O. R. Pols, C. A. Tout, P. P. Eggleton, Z. Han, *MNRAS* **274**, 964 (1995).
61. E. Glebbeek, O. R. Pols, J. R. Hurley, *A&A* **488**, 1007 (2008).
62. J. C. Lombardi, Jr., *et al.*, *ApJ* **640**, 441 (2006).
63. E. Gaburov, J. C. Lombardi, Jr., S. Portegies Zwart, *MNRAS* **402**, 105 (2010).
64. J. C. Lombardi, Jr., *et al.*, *ApJ* **737**, 49 (2011).
65. V. Renvoizé, I. Baraffe, U. Kolb, H. Ritter, *A&A* **389**, 485 (2002).
66. Podsiadlowski, P. 2001, *Evolution of Binary and Multiple Star Systems*, 229, 239
67. U. Munari, *et al.*, *A&A* **474**, 585 (2007).
68. N. Ivanova, P. Podsiadlowski, *Exotic Stars as Challenges to Evolution*, C. A. Tout & W. van Hamme, ed. (2002), vol. 279 of *Astronomical Society of the Pacific Conference Series*, pp. 245–+.

69. P. Podsiadlowski, *NewAstRev* **54**, 39 (2010).
70. A. Rest, *et al.*, *Nature* **482**, 375 (2012).
71. L. Chomiuk, M. S. Povich, *AJ* **142**, 197 (2011).
72. P. Kroupa, *Science* **295**, 82 (2002).
73. M. Politano, M. van der Sluys, R. E. Taam, B. Willems, *ApJ* **720**, 1752 (2010).
74. D.J. Price, *PASA*, **24**, 159 (2007)

**Acknowledgments:** N.I. acknowledges support from the Natural Sciences and Engineering Research Council of Canada and the Canada Research Chairs Program. S.J. acknowledges support from the Chinese Academy of Sciences and National Natural Science Foundation of China. J.L.A.N. acknowledges support from CONACyT. J.C.L. thanks R. Scruggs for useful discussions. This research has been enabled by the use of computing resources provided by WestGrid and Compute/Calcul Canada as well as the Extreme Science and Engineering Discovery Environment (supported by NSF grant OCI-1053575).